Catalytic Reaction Mechanism of Lipoxygenase. A Density Functional Theory Study

Tomasz Borowski[†] **and Ewa Broclawik***[,‡]

Faculty of Chemistry, Jagiellonian University, Ingardena 3, 30-060 Kraków, Poland, and Institute of Catalysis and Surface Chemistry, Polish Academy of Sciences, Niezapominajek 8, 30-239 Kraków, Poland

Received: December 4, 2002; In Final Form: March 3, 2003

The mechanism of the full catalytic cycle for unsaturated fatty acids peroxidation by lipoxygenase has been studied by means of hybrid density functional theory (DFT-B3LYP). The model of the active site in lipoxygenase comprises iron ion coordinated by six-molecule model of the native protein and aqua ligands. Formic anion and formamide are employed to model isoleucine and asparagine, respectively. Histidine ligands are modeled by ammonia molecules. In regards to the substrate, a 2,5-heptadiene molecule is used to model the unsaturated hydrocarbon chain of fatty acids. Our results indicate that the first catalytic step consists of a hydrogen atom transfer from the hydrocarbon to the hydroxide group bound to ferric ion. This process proceeds through an early transition state with the activation energy amounting to 12.1 kcal/mol and the reaction energy being −12.6 kcal/mol. In the next step, the activated substrate, in the form of the diene radical, reacts with a triplet oxygen molecule in an exoergic (−7.8 kcal/mol) process characterized by small activation energy (2.0 kcal/mol). The possibility of an organo-iron intermediate formation has been ruled out by the fact that such a complex is unstable irrespective of the spin state assumed. Similarly, the reduced form of the active site seems not to bind molecular oxygen to any perceptible extent, which in turn remains at variance with the mechanism assuming molecular oxygen activation. The last step of the catalytic reaction involves the peroxy radical reduction by the ferrous form of the active site in lipoxygenase. This process is almost isoenergetic (0.3 kcal/mol) and completes the catalytic cycle. Two possible mechanisms of this last step are discussed with particular attention on the possible catalytic relevance of the so-called purple form.

I. Introduction

Lipoxygenases (LOs) constitute a family of non-heme iron enzymes catalyzing dioxygenation of polyunsaturated fatty acids. Although LOs are widespread in plant and animal kingdoms,[1] soybean lipoxygenase-1 (SLO-1) has become a representative enzyme of the family due to its abundance in seeds. Thus, most of the research has been devoted to this particular lipoxygenase and the general results obtained for SLO-1 are believed to be typical for the whole group of LOs. Hence, most of the scientific literature considering the catalytic mechanism of lipoxygenases rest on the results obtained for SLO-1, and this reason prompted us to focus our research on this LO.

The X-ray crystal structure of SLO-1 has been reported by Boyington et al.[2] and Minor et al.,[3] but as the latter has been resolved to much higher resolution (2.6 vs 1.4 Å), our discussion and models are based on this particular structure (PDB entry: 1YGE) and its further refinement published recently (PDB entry: 1F8N).[4] In the resting form of SLO-1, the active site contains one ferrous ion coordinated by three histidines, C-terminal isoleucine, one water molecule, and a loosely bound asparagine (see Figure 1). On the basis of MCD[5] and EXAFS[6] data, this asparagine ligand has been proposed to form a normal covalent bond with iron ion upon substrate binding or ferrous site oxidation. Thus, it is now widely accepted that the six-coordinated iron site is calatytically relevant. Moreover, the crystal structure of SLO-1 reveals that in the vicinity of the iron site there is no other functional group that might be involved in a catalytic mechanism.

* Corresponding author. E-mail: broclawi@chemia.uj.edu.pl. Fax: 48 12 634-05-15.
[†] Jagiellonian University.
[‡] Polish Academy of Sciences.

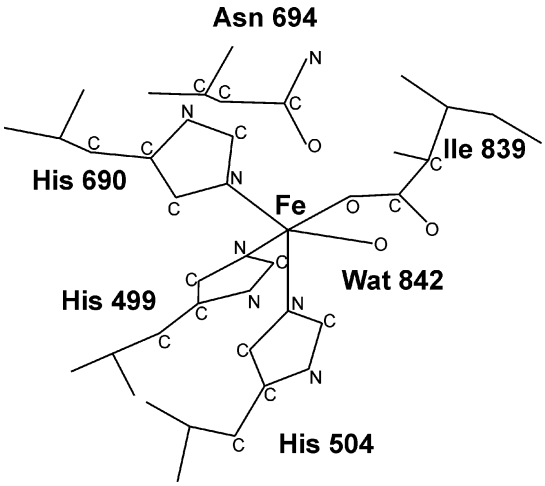

Figure 1. Active site of soybean lipoxygenase (SLO-1) from crystal structure (1YGE).

The basic catalytic reaction of lipoxygenases is a polyunsaturated fatty acids dioxygenation. The reaction catalyzed by SLO-1, in which linoleic acid is oxidized to 13-hydroperoxy-9,11-octadecadienoic acid,13-HPOD (see Figure 2), may serve as an example. The products of this reaction, i.e., fatty acids peroxides, have versatile biological functions,[1,7] among which the best known is the aspect of their serving as precursors in the synthesis of potent inflammatory agents (leukotrienes and lipoxins) in animal organisms.

As regards the catalytic mechanism of LO, three different mechanisms have been proposed in the literature and they are depicted in Figure 3. Below we discuss each of them and present experimental findings in their support.

10.1021/jp027616q CCC: $25.00
Published on Web 04/16/2003

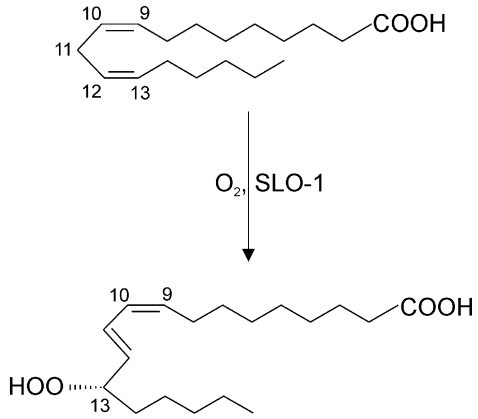

Figure 2. The basic reaction catalyzed by SLO-1: synthesis of 13-HPOD from linoleic acid.

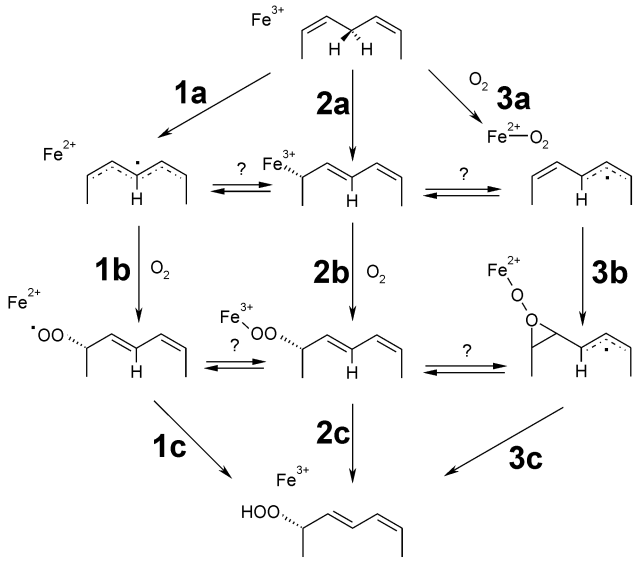

Figure 3. Three different mechanisms proposed for lipoxygenase. From the left: radical, organo-iron, and ene-radical.

The radical mechanism, which involves steps 1a−c shown in Figure 3, assumes that the first step (1a) is the hydrogen atom abstraction from the substrate taking place simultaneously with the active site iron ion reduction. The fact that the hydrogen abstraction requires the ferric form of the enzyme and that it results in the hydrocarbon radical formation is well documented. For example, Schilstra et al.[8] have demonstrated that only the ferric form of LO is catalytically active, while Glickman and Klinman[9] have established that the hydrogen atom abstraction precedes dioxygen binding. Moreover, the presence of carbon-centered radicals forming in the absence of oxygen has been confirmed.[10] In addition, the identity of the carbon-centered radical, which is also present in the purple form solution, has been probed with EPR spectroscopy by Nelson and co-workers.[11] The EPR data have been interpreted in favor of the pentadiene radical that might be slightly twisted around the $C_{10}-C_{11}$ bond (for atom numbering see Figure 2). Because there are no groups capable of abstracting either hydrogen atom or proton from the substrate in the vicinity of the iron site,[3] both the electron and the proton, i.e., the whole hydrogen atom, must be accepted by the iron site. Therefore, it has been argued by Scarrow et al.[6] that the hydroxide group bound to the ferric ion in the active form of LO constitutes a perfect candidate for the hydrogen-abstracting moiety. In the second step of the radical mechanism (step 1b in Figure 3), molecular oxygen reacts with the pentadiene radical and forms the peroxy radical. The presence of the latter radical bound to the enzyme has been confirmed by EPR experiments,[11] and the direct radical−molecular oxygen reaction is consistent with the very high rate for the reaction between molecular oxygen and SLO-1 with a bound carbon-centered radical.[12] In addition, on the basis of regio- and stereochemistry of the products obtained with some point mutants of SLO-1, Knapp et al.[13] have proposed that the stereo- and regioselectivities of SLO-1 are tuned by the enzyme's steric control of the oxygen approach to the radical. In the last step of the radical mechanism (step 1c in Figure 3), the peroxy radical is reduced by the ferrous form of the active site which means the product formation and the ferric active site regeneration. In the radical mechanism the purple form of lipoxygenase is considered to be a catalytically irrelevant byproduct. In addition, all of the oxygen dependent steps in the catalytic reaction have been shown to be reversible.[14]

The organo-iron mechanism (steps 2a−c in Figure 3) proposed by Corey and Nagata[15] assumes that close to the iron site there is some basic group that serves as a proton acceptor site. Thus, the first step of this mechanism (step 2a in Figure 3) comprises the proton shift from the substrate to this basic site and simultaneously the ferric site attack on the forming carbanion. In the second step (step 2b in Figure 3), molecular oxygen reacts with the organo-iron intermediate and forms the peroxy radical−iron site complex. In the last step (step 2c in Figure 3), this complex reacts with the acid, which is coupled with the before-mentioned basis, and forms the product. This organo-iron mechanism very elegantly explains the regio- and stereoselectivities of LO, and the purple form of lipoxygenase turns out to be the catalytic reaction intermediate formed by oxygen insertion into a single organo-iron bond (step 2b in Figure 3). However, in the X-ray crystal structure there are no candidates for the basic site proposed in the mechanism. Moreover, there are no experimental data supporting the organo-iron complex formation. On the other hand, the chemical character of the purple form of lipoxygenase, i.e., the peroxy radical complex with the ferrous site, has been confirmed in spectroscopic[16] and crystallographic[17] experiments.

The ene-radical mechanism, which has been proposed by Nelson and co-workers,[7] is a variation of the radical mechanism. The first step (step 3a in Figure 3), that is, the hydrogen atom abstraction by the ferric site, ends with a vinyl-allyl radical formation. It is supposed that the substrate channel bends in the proximity of the iron site and that causes the twist of the radical formed in this step. Next, the molecular oxygen binds to the ferrous site and thus activated oxygen molecule attacks the vinyl fragment of the radical (step 3b in Figure 3). Because the vinyl fragment of the radical has a closed-shell character, the activated molecule should have properties of the singlet oxygen. While the magnetic susceptibility measurements have indicated that oxygen does not bind to the ferrous active site of LO,[18] the twist of the substrate channel has been confirmed by the X-ray structure.[3] Moreover, the epoxy-like complex formed in the second step of this mechanism (step 3b in Figure 3) could explain the EPR spectra observed for the purple form solution.[19] The authors have also suggested that this complex rearranges into the purple form and that the latter is the catalytic reaction intermediate. The epoxy-like complex and/or purple form decomposition (steps 3c and 2c in Figure 3) completes the catalytic cycle.

Thus, three distinctive mechanisms have been proposed in the literature, but as it is depicted in Figure 3, they may be

interconnected and, therefore, the specific intermediate may have relevance for more than one mechanism.

The first step of the radical and the ene-radical mechanism, i.e., the hydrogen atom abstraction, deserves further attention due to the exceptionally large kinetic isotope effect (KIE) observed for this reaction. Klinman and co-workers have observed[20] that at temperatures above 32 °C the hydrogen abstraction is the rate-limiting step in the lipoxygenase catalysis. Furthermore, the protium/deuterium kinetic isotope effect measured for this step amounts to ca. 80, and this large KIE cannot be explained by the catalytic reaction branching. In addition, the experimentally determined activation enthalpies for this reaction are extremely low (1.2 and 1.6 kcal/mol for protium and deuterium, respectively) and the rate of protium/deuterium Arrhenius prefactors extrapolated to infinite temperature amounts to ca. 30.[21] Measurements in a magnetic field suggest that this large KIE is not caused by the difference in the nuclear magnetic moments in ^{1}H and ^{2}H, i.e., the magnetic origin of KIE has been excluded in this case.[22] Further experimental data obtained by Rickert and Klinman[23] demonstrate that the large KIE is basically of primary character. In other words, stereospecific deuteration at the critical substrate position, i.e., only the transferred hydrogen is substituted, gives kinetic isotope effect on the order of 80. These experimental data have been interpreted as an evidence of a pure under-the-barrier hydrogen atom tunneling being operational for this reaction.[21] Two distinct theoretical models have been proposed for this tunneling mechanism. The first one, due to Moiseyev et al.,[24] assumes that the tunneling process can be modeled with the two-dimensional potential energy surface. The transition state for this process has a "tight" character, which means that the activation energy, including ZPE, is for protium 1.6 times higher than that for deuterium. The second model, proposed recently by Knapp and co-workers,[25] is a nonadiabatic model of the hydrogen atom tunneling. This approach combines Marcus theory for electron transfer with the overlap Franck−Condon factors which determine the light particle tunneling probability, and it has proved to be very successful in explaining the experimental data for SLO-1. Moreover, this theoretical model works equally well for some point mutants of SLO-1 that have been tested along with the wild-type SLO-1 (WT-SLO). The hydrogen atom transfer distance, i.e., the width of the barrier through which the hydrogen tunnels, has been estimated by the authors and for WT-SLO it equals to 0.567 Å.

Taking into account the wealth of possible catalytic pathways for lipoxygenase and the abundance of experimental data it seems that a detailed theoretical investigation of the catalytic reaction mechanism of LO could bring an independent argument in favor of one of the mechanisms present in the literature. Moreover, such study might bring an insight into the geometrical and electronic structures of the catalytically relevant intermediates and transition states. Bearing all this in mind, we have undertaken the DFT-B3LYP study on the peroxidation reaction catalyzed by LOs. The results, which are presented in detail below, indicate that the radical mechanism is employed by LO and that the purple form may also lie on the reaction path. Thus, the organo-iron and ene-radical mechanisms are found to be energetically hardly accessible. Furthermore, the electronic and geometrical structure of the transition state for the critical hydrogen abstraction step may help to comprehend features of the potential energy surface that give rise to the intricate tunneling phenomenon.

II. Methodology

(a) Models of the Active Site and Reactants. The structure of the active site in lipoxygenases has been probed with X-ray crystallography and various spectroscopic techniques. SLO-1 in its resting form contains one ferrous ion per protein molecule, and as the structure solved by Minor et al.[3] reveals, the metal ion is coordinated by three histidines (His499, His504, and His690), one monodentate carboxylate group of the C-terminal isoleucine (Ile839), and one water molecule. The sixth place in a slightly distorted coordinational octahedron is vacant as the nearest asparagine (Asn694) lies too far away (ca. 3 Å) to form a regular bond. The X-ray data have been further supplemented by the near-infrared MCD measurements. Pavlosky and Solomon[26] have shown that resting (ferrous) form of SLO-1 exists in solution as a mixture of two different species. The first one contains pentacoordinated ferrous ion while in the second one the coordinational octahedron is complete. These findings have been interpreted with an assumption that Asn694 is a weak ligand capable to change its position fairly readily. Indeed, our previous calculations[27] have fully supported that interpretation showing that the Fe(II)-Asn bond elongation may be easily compensated by hydrogen bonding of the Asn. Moreover, of mechanistic importance is the fact that the presence of the substrate or low mass alcohols shifts the equilibrium toward six-coordinated form. On the other hand, EXAFS and XANES measurements by Scarrow et al.[28] made for the active (ferric) form of lipoxygenase indicate that in the oxidized lipoxygenase the nearest surrounding of the iron atom remains unchanged upon alcohol addition. Thus, it is now widely accepted that the six-coordinated form of SLO-1 is catalytically relevant and only models of this form need to be taken into account when the catalytic mechanism is pursued.

In our previous study,[27] concerning geometrical and spectral properties of lipoxygenases, moderate-sized and optimized in a vacuum models of the active sites have proved to be reliable. In these models, amino acids from the first coordination sphere of iron ion have been replaced by their most relevant parts. Histidines have been represented by imidazole rings, asparagine by a formamide molecule, and the C-terminal carboxyl group of isoleucine by a formic anion. As in the present study our aim is to elucidate the catalytic reaction mechanism of lipoxygenase, which implies studying many various mechanisms and intermediates, we had to reduce the size of our models further. Thus, in our current model, the ammonia molecules model the imidazole rings of histidines, while asparagine and the C-terminal carboxyl group of isoleucine are represented as previously by a formamide molecule and a formic anion, respectively. Models of similar size and complexity with ammonia molecules representing histidines have been successfully used in Per Siegbahn's group, and it has been found that the electronic structure and properties of the ammonia-containing and the much bigger, imidazole-based models are virtually identical.[29,30] Indeed, our testing calculations done at the B3LYP/LanL2DZ level of theory indicate that the hydrogen atom binding energies calculated for the two models differ by less than 5 kcal/mol and amount to 95.1 and 90.4 kcal/mol for the bigger and the smaller model, respectively. Taking this into account, we conclude that the use of ammonia molecule as a model of histidine is in our case well corroborated. Therefore, in this study, the small model is used exclusively.

In regards to the substrate, the most relevant part of linoleic acid is modeled by a 2,5-heptadiene molecule. Thus, two methyl

groups flank the basic pentadiene moiety in order to ensure that steric effects are properly taken into account when studying for example organo-iron complex formation.

(b) Quantum Chemical Calculations. Quantum chemical calculations presented in this work concern a relatively large number of models for various intermediate species with potential relevance for catalytic activity of lipoxygenase. Thus, the employed quantum chemical methodology had to be a compromise between the high accuracy needed to investigate an intricate electronic structure of the iron center and the cost of necessary calculations for a broad spectrum of structures. Fortunately, DFT provides a wide range of methods that fulfill these demands. For example, the three parameter hybrid exchange-correlation functional due to Becke[31] (B3LYP) has proved to give high quality geometrical and electronic properties for both organic and inorganic compounds. Furthermore, this particular functional has been extensively used in studies on metallo-enzymes giving results in good accord with experimental findings.[29,30] Thus, taking into consideration the reliability of the B3LYP functional, we have employed it in all computations reported below.

Two different basis sets have been used. The first one, the LanL2DZ basis by Ward and Hay,[32,33] is a double-ζ basis set with effective core potential (ECP) replacing inner-shell electrons on Fe atom. For H, C, N, and O atoms, the D95 basis set by Dunning[34] combined with this ECP basis has been employed. This basis set has been used in all geometry optimizations and Hessian computations because it has proved to be good enough for calculating these properties.[29] The second basis set, used only in single-point electronic energy calculations, was the standard 6-311+G(d,p) basis due to Pople. This relatively large basis set of valence triple-ζ quality contains one set of diffuse functions on heavy atoms and one set of polarization functions on all atoms. Thus, all calculations have been done in two steps. In the first one the geometry of a stationary point on potential energy surface has been optimized and the Hessian calculations performed in order to get the zero-point energy (ZPE). Here, the small double-ζ basis set has been employed. In the second step, single-point energy calculation has been done with the large 6-311+G(d,p) basis set. Hence, the reported energies combine the electronic energy calculated for the LanL2DZ geometry at the 6-311+G(d,p) level with the ZPE obtained with the LanL2DZ basis set.

The atomic spin densities and atomic partial charges are taken from the Mulliken population analysis done at the B3LYP/LanL2DZ level of theory.

All first principle computations have been done with *Gaussian 9*8 (revision A.11).[35] Molecular structures have been drawn with the *Cerius2*[36] program by MSI.

III. Results and Discussion

The present section on the results of DFT calculations is divided into five subsections. Each of them covers an elementary step of one of the proposed mechanisms shown in Figure 3. Thus, in subsection III.a the hydrogen atom abstraction is discussed, while in subsection III.b we focus on the possibility of organo-iron compound formation. Subsection III.c covers the topic of oxygen binding and activation by the ferrous form of the active site in lipoxygenase, whereas subsection III.d concerns oxygen binding by activated substrate, i.e., heptadiene radical. The catalytic cycle is completed by the peroxy radical reduction discussed in subsection III.e, in which we also summarize all of our computational results.

(a) Hydrogen Atom Abstraction. All of the three mechanisms shown in Figure 3 assume that the first step of catalytic reaction involves hydrogen atom or proton abstraction from the substrate. However, the structural data suggest that the hydroxyl group bound to ferric ion is the only basis in the active site capable to abstract proton or hydrogen atom from the substrate molecule. Moreover, there is abundant experimental evidence

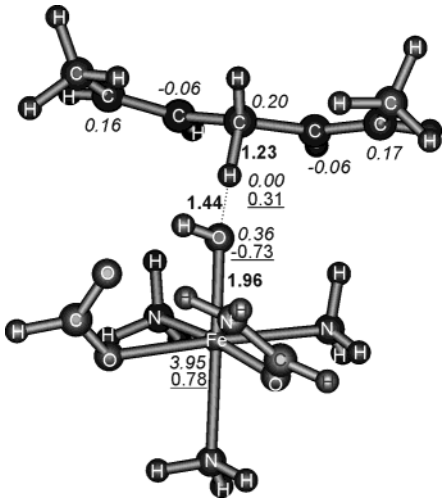

Figure 4. The structure of the optimized transition state for the hydrogen atom abstraction reaction. Bond distances in boldface, spin densities in italics, and atomic charges underlined.

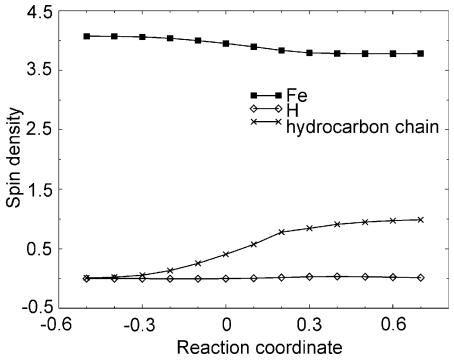

Figure 5. Spin density distribution along the approximate hydrogen atom transfer reaction coordinate. Zero on the reaction coordinate corresponds to the TS geometry.

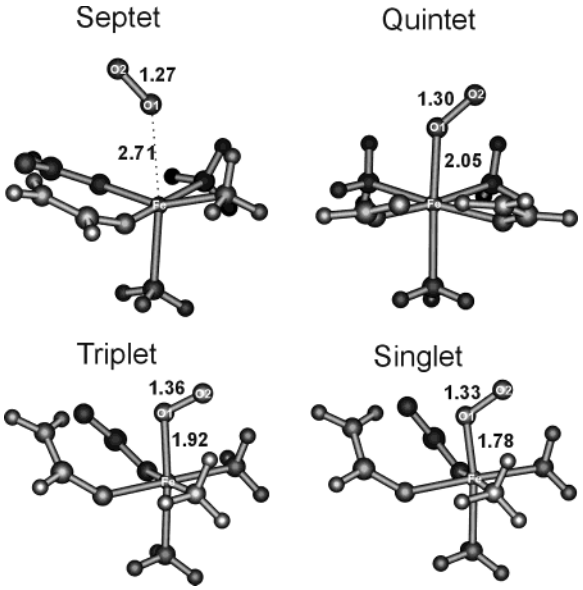

Figure 6. Optimized geometries for the ferrous site−oxygen complexes. Bond distances in bold.

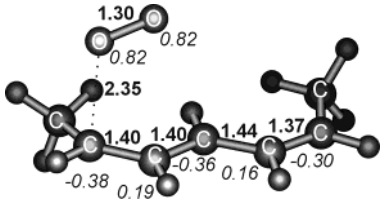

Figure 7. The structure of the optimized transition state for the reaction between molecular oxygen and heptadiene radical. Bond distances in boldface and spin densities in italics.

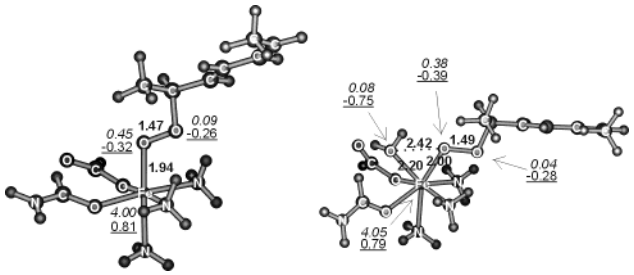

Figure 8. Optimized geometries for six- and seven-coordinated purple form models of SLO-1. Bond distances in boldface, spin densities in italics, and atomic charges underlined.

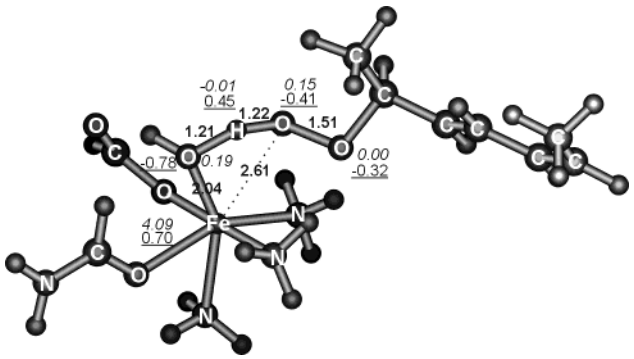

Figure 9. The structure of the optimized transition state for the decomposition reaction of seven-coordinated purple form into the product and the active site. Bond distances in boldface, spin densities in italics, and atomic charges underlined.

for the iron site reduction taking place simultaneously with the hydrogen abstraction. Thus, the very first step in all three mechanisms is actually the same, i.e., the hydrogen atom transfer from the substrate molecule to the hydroxide group bound to the ferric ion (step 1a in Figure 3). Once the hydrogen atom is relocated, the modified organo-iron mechanism (path 2 in Figure 3) assumes radical binding to the ferrous site, while in the ene-radical mechanism (path 3 in Figure 3) molecular oxygen is bound to the ferrous site. Thus, our first objective was to identify and characterize the transition state for the reaction of hydrogen atom transfer between the substrate molecule and the ferric site.

The optimized structure of the transition state for hydrogen shift between the substrate and the ferric site (on the sextet potential energy surface) is depicted in Figure 4, where the most important distances, spin densities, and charges are also shown. Here only the sextet spin state has been examined as the lowest lying quartet excited state of the iron site is placed 33.7 kcal/mol above the sextet ground state. As the hydrogen atom shift reaction is exoergic by as much as 12.6 kcal/mol, the transition state has "early" character. In other words, in the TS structure, the critical C−H bond is only slightly longer compared to that of the substrate molecule (1.229 vs 1.089 Å), and a similar observation holds for the Fe−OH bond distance (1.958 vs 1.822 Å for the TS and the ferric active site, respectively). Furthermore, the oxygen and carbon atoms, together with the hydrogen atom being shifted between them, are perfectly collinear. Thus, the O−C distance equals to the sum of C−H and O··· H distances and amounts to 2.665 Å. From the collinearity of the three atoms and the fact that the normal mode with imaginary frequency corresponds almost exclusively to the hydrogen atom movement, one can easily calculate the approximate hydrogen atom transfer distance as a difference of the O−C separation in the TS structure and the substrate C−H and ferrous active site O−H bond lengths. This approximate value amounts to 0.593 Å and is close to the value of 0.567 Å obtained by Knapp et al.[25] from their nonadiabatic model.

The harmonic analysis performed for the transition state geometry revealed only one imaginary frequency, as it should. Moreover, the analysis of frequencies and zero point energies (ZPE) for natural and deuterated substrate models indicate that the TS is not "tight", as was proposed in the model developed Moiseyev et al.[24] The protium to deuterium substitution at the critical position causes the ZPE to decrease only by 1.3 kcal/mol. Thus, it is apparent that the "tight TS" model is in disagreement with our computational results.

In regards to the electronic properties of the transition state, the calculated activation energy amounts to 12.1 kcal/mol, which might agree very well with the experimentally determined rate of 300 s^{-1} (neglecting thermal and entropic contributions to $\Delta G^{\#}$). However, as it has been described in detail in the Introduction, the isotopic effect measurements clearly demonstrate that the hydrogen atom abstraction from the substrate proceeds through hydrogen atom tunneling. Nevertheless, even the adiabatic transition state demonstrates interesting electronic features and a closer look at them may help to understand the process involved. The spin density and charge distributions depicted in Figure 4 clearly indicate that it is the proton, which is shifted between carbon and oxygen atoms. Both negligible spin density and high partial charge on the transferred moiety strongly support this interpretation. Furthermore, intermediate spin densities on pentadiene moiety and iron ion seem to point out to these two molecular fragments serving as an electron donor and acceptor in the reaction studied here. This conclusion has been further supported by the spin density analysis along a one-dimensional PES scan (see Figure 5). These computations rest on the assumption that in the vicinity of the TS the normal mode corresponding to the only imaginary frequency constitutes a good approximation to the reaction coordinate. Thus, starting from the TS we have distorted the geometry along this normal mode in two opposite directions, and for the geometries obtained in that way we have done single-point calculations followed by a full population analysis. Results of these calculations are presented in Figure 5 where we have plotted spin densities on the critical hydrogen atom, iron ion, and hydrocarbon chain as a function of the approximate reaction coordinate. From Figure 5 it is clearly visible that the proton character of the transferred moiety remains unchanged along the reaction coordinate, while the spin densities on iron and hydrocarbon chain change monotonically, and at the TS geometry, we observe an inflection point on the curves. This picture strongly substantiates the model proposed above which assumes that the whole process of the hydrogen atom abstraction may be seen as an electron transfer from the hydrocarbon chain to the ferric ion accompanied by the proton shift between the carbon and oxygen atoms.

Taking these DFT model results of atomic resolution together with the experimental evidence and the nonadiabatic model developed by Knapp et al.[25] we can now sensibly speculate about the real PES for the hydrogen atom abstraction step catalyzed by lipoxygenase. First of all, our results clearly

demonstrate an intricate character of the hydrogen atom transfer process. Thus, the mechanism can be seen as an electron transfer process accompanied by the proton shift over a relatively short distance. This picture is in accord with the success of the nonadiabatic model of Knapp et al., which is basically a Marcus-like theory for electron-transfer supplemented with Franck−Condon factors so as to take into account light atoms tunneling. However, the relatively low calculated activation energy and the short hydrogen atom transfer distance suggest that the actual substrate−iron site separation might be larger than that in a vacuum. Thus, a slightly longer distance between the substrate and the iron center imposed by the protein might ensure a larger adiabatic activation energy, and the process would then proceed exclusively through hydrogen atom tunneling. That would be in accord with the observation made by Knapp et al. that their calculated hydrogen atom transfer distance, amounting to 0.57 Å, seems to be too small for the fully nonadiabatic process. Moreover, this PES tuning effect caused by the protein envelope would explain the fact that even very well designed functional models of LO are unable to reproduce the large kinetic isotope effect inherent to lipoxygenase catalysis.[37,38] This interpretation of the computational and experimental results should be verifiable by means of mutagenesis experiments and/or carefully designed model systems with, e.g., bulk groups hindering the substrate approach to the iron site.

(b) Organo-Iron Compound. The organo-iron compound formation has been proposed by Corey and Nagata in their original mechanism for lipoxygenase.[15] This intermediate with a sigma bond between the carbon chain and the iron ion has been the crux of their proposal. The presence of this regular bond ensures the required regio- and stereospecificities of the enzyme. Thus, to test the organo-iron hypothesis, we have built an appropriate model in which in place of the hydroxide group coordinating the ferric ion we have put the carbanion chain. The initial Fe−C bond distance has been set to 2.0 Å. Starting from this geometry three separate geometry optimizations have been performed for three possible spin states of the complex: sextet, quartet, and doublet. Irrespective of the spin state assumed, all three optimizations terminated with the Fe−C bond cleaved and the heptadiene radical loosely bound with the ferrous active site. Therefore, it seems that the iron site in lipoxygenase is not apt to bind the activated substrate in the form of the hydrocarbon radical. In light of these results it is very unlikely that the organo-iron intermediate has any mechanistic relevance in the case of lipoxygenase. This conclusion is in accord with lack of any experimental evidence in favor of the organo-iron intermediate formation.

(c) Oxygen Binding to Ferrous Site. In an ene-radical mechanism (path 3 in Figure 3), Nelson et al.[7] have proposed that the unpaired electron is delocalized only over three out of five carbon atoms in the pentadiene unit of the substrate. Therefore, instead of the pentadiene radical, the vinyl-substituted allyl radical is the product of the first step in the catalytic reaction and the vinyl fragment cannot react directly with triplet oxygen. Because the closed-shell vinyl part of it lies in the vicinity of the iron site, the molecular oxygen is proposed to be activated through direct binding to the ferrous site. To check this hypothesis we have optimized four different oxygen−ferrous site complexes. All of them have been built from the model of the ferrous active site by substituting the water ligand with the oxygen molecule. The four models differ in the spin state, and they have the following spin multiplicities: septet, quintet, triplet, and singlet. The optimized structures of these models are depicted in Figure 6, while the most important spin densities together with the relative energies are gathered in Table 1. Inspection of Table 1 shows very clearly that none of the ferrous−oxygen complexes is stable with respect to the ferrous−aqua complex. Moreover, only the septet complex has energy low enough to be taken into consideration. However, in this case the oxygen molecule is only very loosely bound to the iron ion and the oxygen molecule maintains its triplet character (see spin densities in Table 1). The first complex with significant spin density reduction on oxygen atoms, i.e., the quintet complex, has energy much too high to be seriously taken into consideration. Thus, our calculations indicate that the molecular oxygen does not bind to the ferrous active site, and hence, the oxygen activation hypothesis has no support in theoretical calculations. This is in good agreement with the results of magnetic susceptibility measurements[18] that ruled out the possibility of molecular oxygen binding to the native ferrous form of SLO-1.

TABLE 1: Energy of the Substitution Reaction ($Fe-OH_2 + O_2 \rightarrow Fe-O_2 + H_2O$) and Spin Densities for the Studied Ferrous Site−Oxygen Complexes

multiplicity	ΔE [kcal/mol]	spin on O1	spin on O2
7	12.8	0.92	1.06
5	21.0	0.03	−0.24
3	31.9	0.39	0.60
1	42.7	0.00	0.00

(d) Oxygen Binding by Activated Substrate. Having discussed in previous subsections the organo-iron intermediate and the hypothesis of molecular oxygen activation, now we focus on the direct reaction between the organic radical and molecular oxygen. This reaction is exoergic with the reaction energy amounting to −7.8 kcal/mol, and it proceeds through a low-lying transition state. The calculated activation energy equals 2.0 kcal/mol, and the geometry of the TS is depicted in Figure 7. Presented in this figure are bond distances and spin densities for the hydrocarbon chain indicating some localization of the unpaired electron on the carbon attacking molecular oxygen. In addition, the spin density on oxygen atoms is reduced from the free-molecule value (1.0) and manifests the already started oxygen-binding process.

For the vinyl-allyl radical with the constrained relative positions of the vinyl and allyl parts, the approximate activation energy amounts to only 7.8 kcal/mol. Thus, in all cases, the direct reaction between molecular oxygen and the organic radical is much easier than oxygen activation by the ferrous active site. This direct reaction gives as a product the peroxy radical whose presence in the active site of lipoxygenase has been confirmed in EPR experiments.

Since the ene-radical mechanism assumes the existence of an intermediate with an epoxy-like radical coordinating the ferrous active site, we have also investigated the stability of this form of the peroxy radical. Thus, we have optimized the geometry of the allyl radical with the epoxy-like substituent. However, this form has turned out to be very unstable and its energy is 52.8 kcal/mol higher than that for the peroxy radical. Furthermore, the complex formation between this radical and the ferrous active site (see step 3b in Figure 3) has been found to be endoergic by 44.8 kcal/mol. Accordingly, combining this result with the very low oxygen affinity to the ferrous site, it seems to be apparent that the whole ene-radical mechanism is implausible.

On the basis of spectroscopic[16] and X-ray crystallographical[17] data, it is now well established that the peroxy radical may bind to the ferrous active site forming a so-called purple form of lipoxygenase. However, it has been unclear whether this short-

living form has catalytic relevance[17,19] or constitutes only an interesting but mechanistically insignificant byproduct.[13] With these questions in mind we have performed geometry optimization and Hessian calculations for two possible purple form models. In the first one the aqua ligand has been substituted by peroxy radical while in the second one the aqua ligand has been retained. Thus, the two models differ in coordination number, the first one (6C P.F.) has a six- while the second (7C P.F.) a seven-coordinated iron ion. The optimized structures of these two models are presented in Figure 8. The formation reaction energy ($LFe-OH_2 + ROO \rightarrow$ 7C P.F. or 6C P.F. $+ H_2O$) calculated for these two complexes is identical and amounts to −6.0 kcal/mol. Therefore, the generation of the purple form of lipoxygenase is energetically favorable which agrees with the fact that this form is experimentally observed.

(e) Peroxy Radical Reduction. To close the catalytic cycle, the peroxy radical, whose formation has been described in previous subsection, must be reduced by the ferrous form of the active site. This process may proceed either directly, with hydrogen atom shift between the ferrous site and the peroxy radical, or within the first coordination shell[11] of the seven-coordinated purple form (7C P.F.).[39] Both of these possibilities have been examined and the results are presented below.

The direct hydrogen atom transfer between the ferrous site and the peroxy radical has been found to be very slightly endoergic with the reaction energy equaling to 0.3 kcal/mol. Despite many thorough attempts, which we have undertaken with the hope to find the TS for this reaction, we have obtained exclusively a monotonic energy change accompanying the hydrogen atom shift. The lack of the transition state in this case can be rationalized with the argument that this reaction takes place between two open-shell subsystems. Moreover, none of them undergoes any dramatic change in its electronic or geometrical structure in the course of the reaction. Hence, there is no barrier in this case as the presence of the barrier usually manifests significant structure rearrangements.

Alternatively, the last step of the catalytic reaction could proceed through seven-coordinated purple form of lipoxygenase. In the optimized structure of this form, depicted in Figure 8, the aqua and peroxy ligands are so positioned (O−O distance amounts to 2.415 Å) that their arrangement could facilitate the hydrogen atom transfer. The optimized transition state geometry for this process is presented in Figure 9. From the critical interatomic distances it is not difficult to recognize that the Fe−OOR bond breaks simultaneously with the proton shift. The calculated activation energy equals to 10.1 kcal/mol, while the reaction is endoergic with the reaction energy amounting to 6.2 kcal/mol. Thus, the results obtained for the two possible mechanisms of the peroxy radical reduction suggest that the direct peroxy radical reduction is kinetically favorable, while the purple form formation is thermodynamically advantageous. Therefore, if we assume that in the real protein there might be some small energetic barrier for the purple form formation (e.g., associated with peroxy radical dislocation necessary for the Fe−OOR bond forming), then it is tempting to try to explain some experimental observations. For example, in the case of small substrate concentration, the level of the peroxy radical is so small that all of it is processed into the product that is released from the active site, and no purple form is observed. Only if the concentration of the substrate and/or the product ascends, accumulation of the peroxy radical eases the purple form formation. Unfortunately, the energy differences in this region of PES are so small, that this interpretation has to be considered as a tentative one.

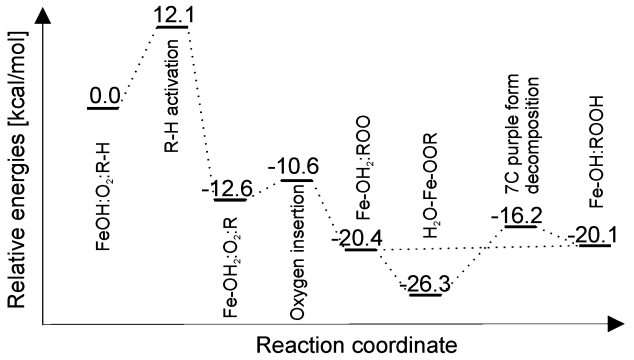

Figure 10. Potential energy surface obtained for the catalytic reaction of SLO-1.

The results of our calculations are summarized in Figure 10, which presents the potential energy surface for the catalytic reaction of lipoxygenase. Upon comparison of Figures 3 and 10 it is clear that this is the radical mechanism that has been indicated by our results. The other two mechanisms have been ruled out with the exception of possible, but rather unlikely, catalytic relevance of the purple form. In summary, the catalytic process starts with the hydrogen atom abstraction from the substrate. This reaction proceeds through hydrogen atom tunneling and is virtually irreversible. This process is also the rate-limiting step of the whole catalytic reaction. The next step consists of molecular oxygen binding to the pentadiene radical and produces the peroxy radical intermediate. In the last step the peroxy radical is reduced by the ferrous active site either directly or through the seven-coordinated purple form, but the latter pathway is less probable. However, the decomposition reaction engaging the seven-coordinated purple form may serve as an explanation of the experimentally observed purple form unstableness. The whole peroxidation process is exoergic and the reaction energy amounts to −20.1 kcal/mol.

IV. Conclusion

The presented DFT results support several well-established experimental findings concerning soybean lipoxygenase (SLO-1). First of all, the hydrogen atom abstraction from the substrate has been found to be the most difficult step in the catalytic cycle. Although the results reported here cannot explain the unusually high kinetic isotope effect for this step, they deny the presence of the "tight" transition state proposed in the model due to Moiseyev et al.[24] Moreover, the established structure and electronic properties of the adiabatic transition state for this process may aid to apprehend why this process is nonadiabatic.

Second, the organo-iron compound formation has been refuted by our results. This finding together with the well-established experimental evidence of iron ion reduction at the first step of the catalytic reaction rules out the organo-iron mechanism proposed by Corey and Nagata.[15]

Furthermore, in agreement with experimental findings, we have found that the ferrous form of active site does not bind molecular oxygen to any perceptible extent. The oxygen molecule binding is so endoergic that the mechanism proposing oxygen activation by the ferrous site may be safely excluded.

In addition, if we assume a 5 kcal/mol energy uncertainty for the DFT calculations, all of the catalytic steps with the only exception of the hydrogen atom abstraction occur to be thermodynamically reversible, which is in good agreement with experimental data.

In light of the results presented here, it seems that the basic catalytic mechanism of lipoxygenase has been recognized.

However, it is also apparent that there is a great deal of further work to be done before we fully comprehend all aspects of lipoxygenase chemistry. One of the questions awaiting an answer concerns the mechanism of monounsaturated fatty acids oxidation, which yields enons instead of the usually observed hydroperoxides.[40] This is the problem we are now working on, and we hope to publish the results soon.

Note Added in Proof. While this work was within the reviewing procedure, Lehnert and Solomon[41] published a similar paper in which they concentrated on the hydrogen atom abstraction step in the lipoxygenase catalytic reaction. Despite of a slightly different computational approach employed in their studies, we believe that the two papers corroborate each other and we refer the interested reader to this paper.

Acknowledgment. This study was sponsored by the Polish State Committee for Scientific Research (Grant 3 T09A 130 19). The computing facilities were supported by a grant from the State Committee for Scientific Research (KBN/SGI_ORIGIN_2000/UJ/042/1999). T.B. thanks Mattias Blomberg for a helpful discussion.

References and Notes

(1) Brash, A. R. *J. Biol. Chem.* **1999**, *274*, 23679.
(2) Boyington, J. C.; Gaffney, B. J.; Amzel, L. M. *Science* **1993**, *260*, 1482.
(3) Minor, W.; Steczko, J.; Stec, B.; Otwinowski, Z.; Bolin, J. T.; Walter, R.; Axelrod, B. *Biochemistry* **1996**, *35*, 10687.
(4) Tomchick, D. R.; Phan, P.; Cymborowski, M.; Minor, W.; Holman, T. R. *Biochemistry* **2001**, *40*, 7509.
(5) Pavlosky, M. A.; Zhang, Y., Westre, T. E.; Gan, Q.-F.; E. Pavel, G.; Campochiaro, C.; Hedman, B.; Hodgson, K. O.; Solomon, E. I. *J. Am. Chem. Soc.* **1995,** *117*, 4316.
(6) Scarrow, R. C.; Trimitsis M. G.; Buck, C. P.; Grove, G. N.; Cowling, R. A.; Nelson, M. J. *Biochemistry* **1994**, *33*, 15023.
(7) Nelson, M. J.; Seitz, S. P. *Curr. Opin. Struct. Biol.* **1994**, *4*, 878.
(8) Schilstra, M. J.; Veldink, G. A.; Vliegenthart J. F. G. *Biochemistry* **1994**, *33*, 3974
(9) Glickman, M. H.; Klinman, J. P. *Biochemistry* **1995**, *34*, 14077
(10) De Groot, J. J. M. C.; Garssen, G. J.; Vliegenthart, J. F. G.; Bolding, J. *Biochim. Biophys. Acta* **1973**, *326*, 279
(11) Nelson, M. J.; Seitz, S. P.; Cowling, R. A. *Biochemistry* **1990**, *29*, 6897.
(12) Glickman, M. H.; Cliff, S.; Thiemens, M.; Klinman, J. P. *J. Am. Chem. Soc.* **1997,** *119*, 11357.
(13) Knapp, M. J.; Seebeck, F. P.; Klinmann J. P. *J. Am. Chem. Soc.* **2001**, *123*, 2931.
(14) Glickman, M. H.; Klinman, J. P. *Biochemistry* **1996**, *35*, 12882.
(15) Corey, E. J.; Nagata, R. *J. Am. Chem. Soc.* **1987**, *109*, 8107.
(16) Nelson, M. J.; Chase, D. B.; Seitz, S. P. *Biochemistry* **1995**, *34*, 6159.
(17) Skrzypczak-Jankun, E.; Bross, R. A.; Carroll, R. T.; Dunham, W. R.; Funk, Jr. M. O. *J. Am. Chem. Soc.* **2001**, *123*, 10814.
(18) Petersson, L.; Slappendel, S.; Vliegenthart, J. F. G. *Biochim. Biophys. Acta* **1985**, *828*, 81.
(19) Nelson, M. J.; Cowling, R. A.; Seitz, S. P. *Biochemistry* **1994**, *33*, 4966.
(20) Glickman, M. H.; Klinman, J. P. *Biochemistry* **1995**, *34*, 14077.
(21) Jonsson, T.; Glickman, M. H.; Sun, S.; Klinman, J. P. *J. Am. Chem. Soc.* **1996,** *118*, 10319.
(22) Hwang, C.-C.; Grissom, C. B. *J. Am. Chem. Soc.* **1994**, *116*, 795.
(23) Rickert, K. W.; Klinman, J. P. *Biochemistry* **1999,** *38*, 12218.
(24) Moiseyev, N.; Rucker, J.; Glickman, M. H. *J. Am. Chem. Soc.* **1997,** *119*, 3853.
(25) Knapp, M. J.; Rickert, K.; Klinman, J. P. *J. Am. Chem. Soc.* **2002**, *124*, 3865.
(26) Pavlosky, M. A.; Solomon, E. I. *J. Am. Chem. Soc.* **1994**, *116*, 11610.
(27) Borowski, T.; Król, M.; Chruszcz, M.; Brocławik, E. *J. Phys. Chem. B* **2001**, *105*, 12212
(28) Scarrow, R. C.; Trimitsis M. G.; Buck, C. P.; Grove, G. N.; Cowling, R. A.; Nelson, M. J. *Biochemistry* **1994**, *33*, 15023.
(29) Blomberg, M. R. A.; Siegbahn, P. E. M. *J. Phys. Chem. B* **2001**, *105*, 9375
(30) Siegbahn, P. E. M.; Blomberg, M. R. A. *Chem. Rev.* **2000**, *100*, 421
(31) Becke, A. D. *J. Chem. Phys*. **1993**, *98*, 5648.
(32) Hay, P. J.; Wadt, W. R. *J. Chem. Phys*. **1985**, *82*, 270.
(33) Hay, P. J.; Wadt, W. R. *J. Chem. Phys*. **1985**, *82*, 299.
(34) Dunning, T. H.; Hay, P. J., Jr. In *Modern Theoretical Chemistry*; H. F. Schafer, H. F., III, Ed.; Plenum: New York, 1976
(35) Frisch, M. J.; Trucks, G. W.; Schlegel, H. B.; Scuseria, G. E.; Robb, M. A.;. Cheeseman, J. R.; Zakrzewski, V. G.; Montgomery, J. A.; Stratmann, R. E.; Burant, J. C.; Dapprich, S.; Millam, J. M.; Daniels, A. D.; Kudin, K. N.; Strain, M. C.; Farkas, O.; Tomasi, J.; Barone, V.; Cossi, M.; Cammi, R.; Mennucci, B.; Pomelli, C.; Adamo, C.; Clifford, S.; Ochterski, J.; Petersson, G. A.; Ayala, P. Y.; Cui, Q.; Morokuma, K.; Malick, D. K.; Rabuck, A. D.; Raghavachari, K.; Foresman, J. B.; Cioslowski, J.; Ortiz, J. V.; Stefanov, B. B.; Liu, G.; Liashenko, A.; Piskorz, P.; Komaromi, I.; Gomperts, R.; Martin, R. L.; Fox, D. J.; Keith, T.; Al-Laham, M. A.; Peng, C. Y.; Nanayakkara, A.; Gonzalez, C.; Challacombe, M.; Gill, P. M. W.; Johnson, B. G.; Chen, W.; Wong, M. W.; Andres, J. L.; Head-Gordon, M.; Replogle, E. S.; Pople, J. A. *Gaussian 98*, revision A.9; Gaussian, Inc.: Pittsburgh, PA.
(36) *Cerius2 Modeling Environment*, release 4.5; Molecular Simulations, Inc.: San Diego, CA, 2000.
(37) Jonas, R. T.; Stack, T. D. P. *J. Am. Chem. Soc.* **1997,** *119*, 8566
(38) Goldsmith, C. R.; Jonas, R. T.; Stack, T. D. P. *J. Am. Chem. Soc.* **2002,** *124*, 83
(39) Wada, A.; Ogo, S.; Watanabe, Y.; Mukai, M.; Kitagawa, T.; Jitsukawa, K.; Masuda, H.; Einaga, H. *Inorg. Chem.* **1999**, *38*, 3592.
(40) Clapp, C. H.; Senchak, S. E.; Stover, T. J.; Potter, T. C.; Findeis, P. M.; Novak M. J. *J. Am. Chem. Soc.* **2001**, *123*, 747.
(41) Lehnert, N.; Solomon, E. I. *J. Biol. Inorg. Chem.* **2003**, *8*, 294.